

BEYOND CLASSIFICATION ACCURACY: NEURAL-MEDBENCH AND THE NEED FOR DEEPER REASONING BENCHMARKS

Miao Jing^{†,1,5}, Mengting Jia^{†,1}, Junling Lin², Zhongxia Shen³, Lijun Wang⁴, Yuanyuan Peng⁴,
Huan Gao¹, Mingkun Xu¹, Shangyang Li^{1,6,*}

¹Guangdong Institute of Intelligence Science and Technology, Hengqin, Zhuhai, Guangdong, China

²Beijing Chaoyang Hospital, Capital Medical University, Beijing, China

³Sleep Medical Center of Huzhou Third Municipal Hospital,
the Affiliated Hospital of Wenzhou Medical University, Huzhou, China

⁴Shenzhen Hospital (Futian) of Guangzhou University of Chinese Medicine,
Shenzhen, Guangdong, China

⁵University of Macau, Macau, China

⁶Academy for Advanced Interdisciplinary Studies, Peking University, Beijing, China

[†]These authors contributed equally to this work.

*syli@pku.edu.cn

ABSTRACT

Recent advances in vision-language models (VLMs) have achieved remarkable performance on standard medical benchmarks, yet their true clinical reasoning ability remains unclear. Existing datasets predominantly emphasize classification accuracy, creating an evaluation illusion in which models appear proficient while still failing at high-stakes diagnostic reasoning. We introduce *Neural-MedBench*, a compact yet reasoning-intensive benchmark specifically designed to probe the limits of multimodal clinical reasoning in neurology. *Neural-MedBench* integrates multi-sequence MRI scans, structured electronic health records, and clinical notes, and encompasses three core task families: differential diagnosis, lesion recognition, and rationale generation. To ensure reliable evaluation, we develop a hybrid scoring pipeline that combines LLM-based graders, clinician validation, and semantic similarity metrics. Through systematic evaluation of state-of-the-art VLMs, including GPT-4o, Claude-4, and MedGemma, we observe a sharp performance drop compared to conventional datasets. Error analysis shows that reasoning failures, rather than perceptual errors, dominate model shortcomings. Our findings highlight the necessity of a Two-Axis Evaluation Framework: breadth-oriented large datasets for statistical generalization, and depth-oriented, compact benchmarks such as *Neural-MedBench* for reasoning fidelity. We release *Neural-MedBench* at <https://neuromedbench.github.io/> as an open and extensible diagnostic testbed, which guides the expansion of future benchmarks and enables rigorous yet cost-effective assessment of clinically trustworthy AI.

1 INTRODUCTION

Recent advances in vision-language models (VLMs) have led to striking improvements across a wide range of medical AI tasks. On standard benchmarks such as MedMNIST v2 Yang et al. (2023) and MultiMedQA Zhou et al. (2024), state-of-the-art models achieve near-human or even superhuman performance in label prediction and image-text alignment. These results have created an impression that medical VLMs are nearing clinical readiness. Yet, as the clinical reasoning literature has recently underscored Schwartzstein (2024), safe and effective diagnostic practice, especially in high-stakes fields such as neurology, demands more than classification accuracy: it requires multimodal synthesis, ambiguity resolution, and the capacity to justify conclusions in a manner consistent with clinical logic.

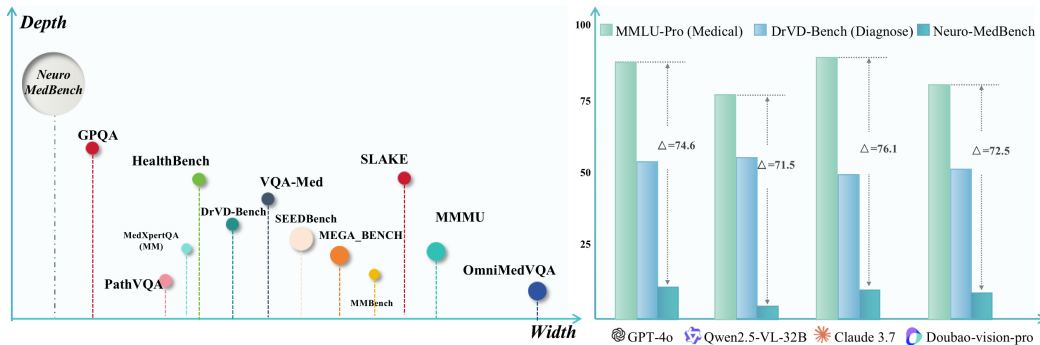


Figure 1: **Conceptual Positioning of Neural-MedBench and Empirical Evidence of the Evaluation Illusion.** (Left) An illustrative mapping of existing medical VLM benchmarks along the proposed axes of Breadth (dataset size and diversity) and Depth (reasoning complexity). Most benchmarks occupy the high-Breadth, low-Depth space, leaving a critical gap in high-Depth evaluation, which Neural-MedBench is designed to fill. (Right) Performance of leading VLMs on two Breadth-Axis benchmarks (MMLU-Pro and DrVD-Bench) versus our Depth-Axis benchmark (Neural-MedBench). The stark performance drop on Neural-MedBench provides clear empirical evidence of the “evaluation illusion” and the disconnect between the two evaluation axes. Table.2 shows full results.

Current benchmarks, despite their scale, rarely capture these aspects. We argue that this discrepancy creates an *evaluation illusion*, a misleading sense of model capability, where strong performance on shallow benchmarks obscures deep weaknesses in reasoning fidelity and clinical trustworthiness.

To address this gap, we propose a new perspective on evaluation: a **Two-Axis Evaluation Framework** for medical AI. Along the first axis, **Breadth**, large-scale datasets assess statistical generalization and coverage across populations and conditions. This is where almost all existing benchmarks operate. However, recent work such as DiagnosisArena Zhu et al. (2025) has shown that relying solely on such breadth-oriented evaluations leads to overestimation of model capability, as they fail to capture true clinical reasoning challenges. Along the second axis, **Depth**, compact but diagnostically complex, expert-curated benchmarks assess reasoning fidelity, forcing models to integrate multimodal signals, reason under uncertainty, and provide structured justifications, an approach that echoes trends in MedAgentsBench Tang et al. (2025). Importantly, we hypothesize that these axes are largely uncorrelated: success on breadth benchmarks does not guarantee competence in depth scenarios. This hypothesis is supported by findings that even expert LLMs struggle with self-awareness and metacognitive reasoning on challenging cases, as shown in MetaMedQA Griot et al. (2025). A complete picture of model readiness therefore requires evaluation along both dimensions.

To operationalize the Depth axis in clinical neurology, we introduce Neural-MedBench, a diagnostic benchmark deliberately designed as a “stress test.” Neural-MedBench comprises 120 expert-annotated multimodal cases, including multi-sequence MRI scans, structured electronic health records (EHRs), and clinical narratives, yielding 200 reasoning-intensive tasks. Its design mirrors practices in medical education, such as Objective Structured Clinical Examinations (OSCEs), where carefully constructed cases are used to assess reasoning skills under uncertainty Geathers et al. (2025); Siegelman et al. (2024). Unlike prior resources focused on breadth, Neural-MedBench is compact by design, prioritizing reasoning density over volume, enabling cost-effective yet high-signal evaluation of clinical reasoning.

Our evaluation of leading models, including GPT-4o, Claude 4, and MedGemma, reveals a striking pattern: models that excel on large-scale benchmarks fail systematically on Neural-MedBench. Error analysis shows that these failures stem not from perception or lexical mismatch, but rather from breakdowns in clinical reasoning, limitations that remain hidden under existing evaluation paradigms. This disconnect provides the first empirical evidence for the independence of the two axes, underscoring the urgent need for benchmarks that explicitly capture reasoning depth.

This work makes the following contributions:

- We propose the Two-Axis Evaluation Framework, arguing that trustworthy clinical AI requires complementary assessments of both breadth (statistical generalization) and depth (reasoning fidelity).
- We release `Neural-MedBench`, the first neurology-focused benchmark explicitly designed to operationalize the Depth axis, comprising 120 multimodal, expert-curated diagnostic cases with 200 reasoning-intensive tasks.
- We provide empirical evidence of the disconnect between breadth and depth, showing that state-of-the-art VLMs fail primarily at reasoning, despite strong performance on existing large-scale datasets.
- We present a systematic error analysis and a human performance baseline to contextualize model results, and we release `Neural-MedBench` as an open, extensible resource with a public leaderboard and roadmap for expansion.

2 RELATED WORK

2.1 MEDICAL VLM BENCHMARKS

A wide range of benchmarks have been developed for evaluating medical VLMs. Early datasets such as ChestX-ray14 Wang et al. (2017), CheXpert Irvin et al. (2019), and MIMIC-CXR Johnson et al. (2019) primarily enabled large-scale classification and report generation. Organ- or disease-specific challenges—including LUNA for pulmonary nodules Setio et al. (2017), LiTS for liver tumors Bilic et al. (2019), BraTS for brain tumors Menze et al. (2015), and ISLES for stroke Winzeck et al. (2017)—expanded evaluation to segmentation and lesion characterization. More recent multimodal benchmarks target richer tasks: ROCO v2 Rückert et al. (2024) for radiology captioning, RadGraph Jain et al. (2021) for entity–relation extraction, and MedFMC Zhang et al. (2023) for federated multi-center classification. VQA-style benchmarks, such as VQA-RAD Lau et al. (2018), PathVQA He et al. (2020), and OmniMedVQA Hu et al. (2024), test text–image reasoning but often rely on templated questions, limiting their coverage of authentic diagnostic challenges. Recent meta-benchmarks (e.g., Rad-Bench Kuo et al. (2024), DiagnosisArena Zhu et al. (2025), MedAgents-Bench Tang et al. (2025)) have emphasized comprehensiveness, yet remain breadth-oriented: they focus on scale and diversity rather than probing reasoning under uncertainty.

In contrast, `Neural-MedBench` explicitly operationalizes the *Depth axis* of evaluation. By curating 120 multimodal, diagnostically complex neurology cases into 200 reasoning-intensive tasks, it emphasizes reasoning fidelity over volume. This design mirrors clinical examinations such as OSCEs, and captures underexplored challenges like multi-lesion differential diagnosis, contextual interpretation, and longitudinal integration across MRI sequences.

2.2 VLM EVALUATION METHODOLOGIES

Medical VLMs are typically evaluated via three strategies: reference-based, reference-free, or hybrid metrics. Traditional reference-based methods include BLEU, ROUGE, and CIDEr for surface overlap, as well as semantic similarity scores such as BERTScore Zhang et al. (2019), CLIPScore Hessel et al. (2021), and domain-specific adaptations like CheXbert Smit et al. (2020) or RadGraph-F1 Jain et al. (2021). While scalable, these methods cannot assure that generated outputs are clinically grounded. Reference-free approaches, such as saliency attribution (e.g., Grad-CAM Selvaraju et al. (2020)) or image–text alignment tests, serve as indirect proxies for reasoning but lack explanatory power. More recent frameworks have introduced LLM-based grading systems for evaluating factual accuracy and reasoning plausibility in free-form clinical responses. For example, the Expert-of-Experts Verification and Alignment (EVAL) framework streamlines clinician-led evaluation in bleeding scenarios Smith et al. (2025), while LLMEval-Med combines expert-designed checklists with LLM-as-Judge dynamics to improve reliability in medical QA and reasoning tasks Zhang et al. (2025); Zhi et al. (2025). Despite their automation advantages, these approaches remain subject to ongoing reliability validation.

`Neural-MedBench` employs a hybrid evaluation strategy: semantic fidelity is quantified using BERTScore, while clinical reasoning is scored via an LLM-based evaluator calibrated with neurologist

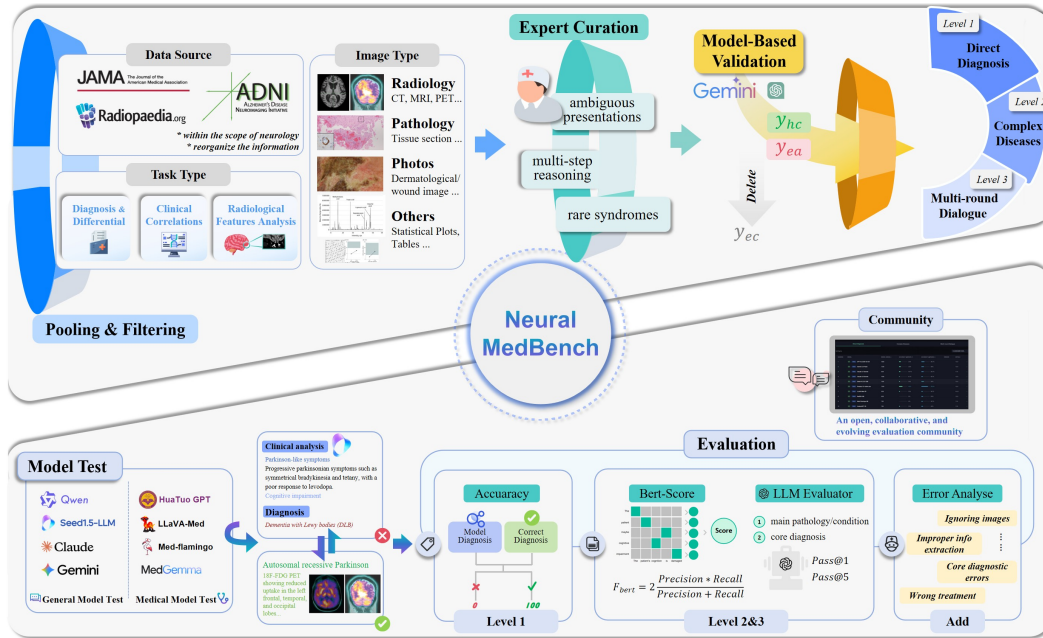


Figure 2: **Overview of Neural-MedBench.** The workflow begins with pooling and filtering data from diverse clinical sources, followed by a multi-stage expert curation and model-based validation pipeline to select for diagnostically complex cases. The resulting benchmark is used to test a cohort of models, whose outputs are assessed via a hybrid evaluation suite including accuracy, semantic similarity, and a clinician-validated LLM grader.

review. This design allows scalable yet clinically faithful assessment of both “what” is predicted and “why,” exposing nuanced failure modes that conventional metrics tend to overlook.

3 NEURAL-MEDBENCH

Design Philosophy and Motivation. As established in our proposal for a Two-Axis Evaluation Framework, current medical benchmarks overwhelmingly emphasize Breadth, rewarding statistical generalization but failing to probe deep, integrative reasoning. To address this gap, Neural-MedBench was conceived to operationalize the Depth axis. Its design philosophy is therefore fundamentally different from large-scale datasets.

Instead of prioritizing data volume, we prioritize reasoning density. Our goal was to create a compact but diagnostically rich “stress test,” inspired by high-stakes clinical examinations like OSCEs, where the ability to synthesize, reason, and justify is paramount. This approach, illustrated in Figure 2, allows for a rigorous yet cost-efficient evaluation of the core clinical reasoning capabilities that remain under-assessed by existing resources.

Case Sources and Curation. We curated 120 authentic neurology cases from multiple rigorously vetted sources: ADNI and OASIS (research cohorts), Radiopaedia (expert-verified imaging cases), and peer-reviewed case reports (e.g., JAMA Neurology). These sources span both common diseases (e.g., Alzheimer’s disease, ischemic stroke, epilepsy) and rare or diagnostically complex conditions (e.g., autoimmune encephalitis, CNS infections).

The final 120 cases were selected from an initial pool of over 2,000 candidates using a funnel-shaped, multi-stage pipeline: (1) *Initial screening* retained only cases with sufficient multimodal completeness (e.g., imaging, neuropsychological scores, patient histories); (2) *Expert curation* by two senior neurologists and one neuroradiologist, who reviewed cases for plausibility, diagnostic complexity, and educational value; (3) *Annotation* of ground-truth answers, including final diagnosis, differential diagnoses, lesion characterization, and explanatory reasoning; (4) *Consensus review and*

Level 1

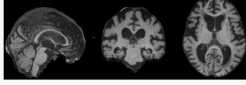
...reported at least one first-degree relative with cognitive impairment, and the father was reported to have cognitive impairment. The patient was taking medication, with a total of 10 medications recorded in a single visit. Reported current use of nonsteroidal anti-inflammatory drugs, anticoagulants or antiplatelet drugs, antidepressants, FDA-approved drugs for the treatment of Alzheimer's disease symptoms....

In addition, she had a history of hypertension, but no history of diabetes, heart disease or stroke, and had recent insomnia....

In terms of lifestyle and behavior, she had drunk alcohol, had not smoked in the past 30 daysand no emotional incontinence was reported....

Subject's blood pressure (sitting) systolic pressure was 118, and the subject's blood pressure (sitting) diastolic pressure was 61. Anxiety occurred in the past few months. GDS total score was 2

Ref: case_id=1(English)



Diagnose the patient's disease.

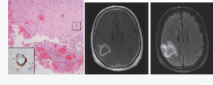
Reference

Alzheimer's disease

Level 2

...intermittent headaches for several weeks, which progressed to severe persistent headaches with pain in the right eye. The patient had hypertension, hyperlipidemia, diabetes mellitus, and atrial fibrillation.... Neurologic examination revealed disorientation, short-term memory impairment, and left arm supination... ..Cerebrospinal fluid (CSF) examination showed normal red blood cell count, protein and glucose levels, and a mildly elevated white blood cell count of 11 cells/ μ L....

What needs to be done next?



Reference

Surgical biopsy of temporoparietal lesionsMRI shows a large T2 hyperintense lesion in the right temporoparietal region with increased DWI signal (decreased apparent diffusion coefficient), low susceptibility-weighted imaging signal, increased T1 signal intensity within and around the lesion, and an enhancing rim and leptomeningeal enhancement. A smaller satellite lesion with similar MRI features is seen below the right anterior temporal lobe. CNS rim-enhancing lesions are accompanied by increased DWI signal and decreased apparent diffusion coefficient... ..The patient's clinical and imaging features are more consistent with cerebral amyloid angiopathy-related inflammation (CAA-ri). The key to a definitive diagnosis is the need for further lesion biopsy.

Level 3

Presents to ED with confusion and word finding difficulties. External CT - left MCA infarct with edema.

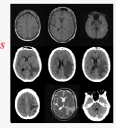
Patient Data
Age: 75 years
Gender: Male

Q1: What is the most likely diagnosis based on the brain imaging?

Q2: What features in the image support the presence of vasogenic edema?

Q3: Based on the imaging features, does this lesion more likely represent a primary brain tumor or a metastasis?

Ref: case_id=17(English)



Reference

The imaging findings are most consistent with a solitary brain metastasis in the left parieto-occipital region, likely from a lung primary, given the homogeneously enhancing intra-axial mass with surrounding vasogenic edema in an elderly patient.

There is low attenuation (on CT) or high T2/FLAIR signal (on MRI) in the white matter surrounding the mass, indicating vasogenic edema

The lesion is more consistent with a metastasis. It is a homogeneously enhancing cortical/subcortical mass with well-circumscribed lobulated borders, associated with extensive vasogenic edema, and without features like

Figure 3: Examples of questions and their reference answers in Neural-MedBench, illustrating typical reasoning tasks.

challenge validation, where disagreements were resolved through discussion, and trivial cases filtered out using baseline models, ensuring each retained case posed a meaningful diagnostic challenge.

This rigorous process ensures that ground truths are not merely single labels but structured narratives that model how neurologists articulate reasoning. Each case supports on average 2 reasoning tasks (200 tasks in total), spanning direct diagnosis, complex disease inference, and multi-turn dialogue. This compact yet high-density design prioritizes diagnostic richness and evaluation efficiency, enabling fine-grained reasoning assessment without the prohibitive annotation and compute costs of large-scale datasets.

Task Families and Difficulty Stratification. From the curated cases, we derived 200 reasoning-intensive tasks, grouped into three core families:

Task Family	Description
<i>Differential Diagnosis</i>	Given imaging and patient history, models must provide a ranked diagnostic hypothesis with justification.
<i>Lesion Recognition</i>	Identify lesion type and location, testing multimodal spatial reasoning.
<i>Rationale Generation</i>	Generate explanatory reasoning for diagnostic choices, mirroring case discussions or board exams.

To probe model reasoning at different depths, these tasks are further stratified into three difficulty levels (see examples in Fig. 3):

- **Level 1 (Direct):** Straightforward cases with clear diagnostic cues.
- **Level 2 (Complex):** Ambiguous presentations or rare neurological diseases requiring deeper inference.
- **Level 3 (Multi-turn):** Simulated consult-style dialogue requiring iterative reasoning and multimodal synthesis.

This design provides a controlled lens into how models scale from factual recall to higher-order clinical reasoning.

Evaluation Protocol. Evaluating deep clinical reasoning is notoriously resource-intensive. To address this, Neural-MedBench introduces a scalable, hybrid evaluation pipeline that is rigorously validated by clinicians, but fully automatable for community use. The protocol consists of two stages:

Stage 1: Grader Validation. The core of our protocol is a dedicated LLM-based grader, guided by detailed, neurology-specific rubrics. To ensure this automated grader serves as a reliable proxy for expert judgment, we performed a rigorous clinician-in-the-loop validation. A panel of board-certified neurologists independently scored a large subset of model outputs using the same rubric. We found a very high correlation between the LLM grader’s scores and the consensus of human experts (e.g., Pearson’s $r > 0.9$), scientifically validating our grader as a robust instrument for automated assessment.

Stage 2: Automated Community Evaluation. Following this one-time, intensive validation, the clinically-calibrated LLM grader is released as part of the benchmark. This allows any researcher to evaluate a new model in a fully automated fashion, without requiring access to clinicians. Users can simply run their model on `Neural-MedBench` and use our provided, validated grader to obtain scores that are highly correlated with expert neurological assessment.

To further contextualize results from this automated pipeline, we also establish a human performance baseline by evaluating clinicians of varying expertise on the benchmark. This crucial addition anchors all model scores, providing a clear, realistic measure of the gap between current AI capabilities and human-level clinical reasoning. This two-stage protocol thus offers the best of both worlds: the gold-standard rigor of clinician validation and the scalability of automated evaluation.

Dataset Analysis. Table 1 summarizes task statistics. Text inputs were normalized in length to control for spurious effects of input size on model performance. Imaging data include balanced representation of T1, T2, FLAIR, and CT modalities. Each difficulty tier contains both common and rare pathologies, ensuring robustness tests beyond frequency bias.

Table 1: Text Lengths and Image Pixels by Subset

Subset	Token Chinese	Token English	Image Pixel (x10,000)
Level 1	374	225	535
Level 2	504	309	145
Level 3	67	37	1147

Summary. By integrating multimodal data, stratified diagnostic difficulty, structured reasoning targets, and a cost-efficient hybrid evaluation protocol, `Neural-MedBench` operationalizes the Depth axis of clinical AI evaluation. It complements large-scale breadth benchmarks with a compact, reproducible, and extensible testbed for probing reasoning fidelity, advancing toward clinically trustworthy multimodal AI.

4 EXPERIMENTAL SETUP

Our experimental setup is designed to comprehensively assess the clinical reasoning capabilities of state-of-the-art VLMs on `Neural-MedBench`, and to contextualize their performance against a realistic human baseline.

4.1 MODELS BENCHMARKED

We evaluate 13 representative VLMs spanning three categories, all in a zero-shot setting to probe intrinsic reasoning capabilities without task-specific fine-tuning:

We benchmark three categories of models to provide a comprehensive view of current VLM capabilities. First, we include proprietary frontier systems with strong multimodal reasoning ability, namely **GPT-4o** OpenAI (2024) and **Gemini** Comanici et al. (2025), which serve as reference baselines. Second, we evaluate powerful open-source generalist models such as **Claude** Anthropic (2024), **Doubao** Team (2024), **Qwen-VL-Plus** Bai et al. (2023). Finally, to assess the effect of domain-specific adaptation, we benchmark medical-specialized VLMs including **LLaVA-Med** Li et al. (2023), **RadFM** Wu et al. (2023), **Med-Flamingo** Moor et al. (2023) and **MedGemma** Sellergren et al. (2025), which represent current efforts to tailor VLMs for clinical applications. A full list of models, versions, and hyperparameters is provided in Appendix C.

4.2 HUMAN PERFORMANCE BASELINE

To establish a realistic anchor for task difficulty, we conducted a human evaluation with two clinician groups: Medical Students ($n = 5$) and Senior Physicians ($n = 5$). Each participant completed the entire set of 200 tasks, blinded to both model outputs and gold-standard answers. All responses were scored using the same evaluation protocol as applied to the models, ensuring a direct and fair human-model comparison.

4.3 TASK AND PROMPTING STRATEGY

To simulate clinical consultations, we adopt a structured role-prompting approach. Each model is initialized as an “experienced neurologist” to encourage adherence to medical reasoning and terminology. Tasks are presented in full, combining textual narratives, structured patient history, and imaging (MRI/CT encoded in base64). Full prompt templates are detailed in Appendix B.

4.4 EVALUATION METRICS

Given the multi-faceted nature of clinical reasoning, we employ a suite of complementary metrics:

- **Diagnostic Accuracy (pass@k):** For tasks with definitive outcomes, we report top-1 (pass@1) and top-5 (pass@5) accuracy. The latter measures whether the correct diagnosis appears within a model’s differential.
- **Semantic Fidelity (BERTScore):** Used for free-form rationale generation, capturing semantic alignment between model outputs and expert references.
- **Reasoning Fidelity (LLM Grader):** A clinically calibrated GPT-4o grader evaluates correctness, logical coherence, and evidence grounding (see Section 5.2).
- **Error Taxonomy:** To understand failure modes, incorrect responses were manually annotated by neurologists into five categories: *Perceptual Failure*, *Reasoning Failure*, *Knowledge Gap*, *Grounding Error*, and *Visual Hallucination*.

This combination of automated metrics, human baselines, and error analysis provides a rigorous and clinically grounded evaluation protocol.

5 EXPERIMENTAL RESULTS AND ANALYSIS

Our experimental analysis is structured to answer three central questions: (1) How do state-of-the-art VLMs perform on a Depth-Axis benchmark like *Neural-MedBench*, and does this performance align with their success on Breadth-Axis benchmarks? (2) How large is the performance gap between these models and practicing human clinicians? (3) What are the primary underlying reasons for model failures in complex clinical reasoning?

5.1 OVERALL PERFORMANCE: A STARK DISCONNECT BETWEEN BREADTH AND DEPTH

We evaluated a diverse cohort of VLMs on all 200 tasks in *Neural-MedBench*, with full results in Table 2. The findings reveal a profound difficulty that stands in stark contrast to conventional benchmarks. Across all models, pass@1 accuracy remains strikingly low, with even the top-performing specialized model *MedGemma-27B-it* only reaching 30.0% on the simplest *Direct Diagnosis* tasks. Performance plummets on more complex subsets, averaging below 15% for most models, a stark contrast to the Senior Physician’s performance of over 35% on the same tasks. Allowing for five attempts (pass@5) improves scores, with the generalist model *Gemini 2.5-Flash* achieving the highest score of 46.7%. However, no model consistently surpasses the 50% mark, indicating that the correct diagnosis is often not even within their top considerations.

This stark performance drop provides the first empirical evidence for our central hypothesis: the two evaluation axes (Breadth and Depth) are largely uncorrelated. To visualize this “evaluation illusion,” Figure 1 contrasts the high scores on a typical Breadth-Axis benchmark against the low scores on *Neural-MedBench*, demonstrating that success in pattern recognition does not translate to competence in deep clinical reasoning.

Table 2: Evaluation metrics across different models and tasks

Models	Direct diagnosis		Complex diseases			Multi-round dialogue		
	pass@1 [%] (n)	pass@5 [%] (n)	BertScore	pass@1[%] (n)	pass@5 [%] (n)	BertScore	pass@1 [%] (n)	pass@5 [%] (n)
Base VLMs								
GPT-4o 2025-03-26	20.0 (6)	36.7 (11)	0.70	8.3 (5)	40.0 (24)	0.73	8.5 (17)	16.5 (33)
Gemini 2.5-Flash	<u>26.7 (8)</u>	46.7 (14)	0.76	<u>13.3 (8)</u>	35.0 (21)	0.68	10.5 (21)	18.5 (37)
General VLMs								
Gemini 2.0-Flash	20.0 (6)	30.0 (9)	0.68	11.7 (7)	23.3 (14)	0.67	<u>9.0 (18)</u>	16.0 (32)
Claude 4.0-Sonnet	16.7 (5)	<u>43.3 (13)</u>	0.78	<u>13.3 (8)</u>	31.6 (19)	0.77	6.5 (13)	<u>18.0 (36)</u>
Claude 3.7 Sonnet	16.7 (5)	26.7 (8)	0.73	8.3 (5)	31.7 (19)	0.66	7.5 (15)	12.0 (24)
Claude 3.5 Sonnet	6.7 (2)	16.7 (5)	0.68	8.3 (5)	18.3 (11)	0.66	7.0 (14)	10.5 (21)
Qwen-VL-2.5	10.0 (3)	30.0 (9)	<u>0.79</u>	5.0 (3)	21.7 (13)	0.69	4.0 (8)	10.0 (20)
Doubao-1.5-vision-pro	6.7 (2)	40.0 (12)	0.64	10.0 (6)	13.3 (8)	0.63	5.5 (11)	11.5 (23)
Medical VLMs								
LLaVA-Med	10.0 (3)	16.7 (5)	0.66	10.0 (6)	28.3 (17)	0.69	6.0 (12)	13.0 (26)
MedGemma-27B-it	30.0 (9)	36.7 (11)	0.80	18.3 (11)	<u>38.3 (23)</u>	<u>0.75</u>	10.5 (21)	15.5 (31)
RadFM	0.0 (0)	20.0 (6)	0.62	3.3 (2)	13.3 (8)	0.67	2.5 (5)	6.0 (12)
Med-Flamingo	0.0 (0)	16.7 (5)	0.67	3.3 (2)	10.0 (6)	0.66	1.5 (3)	10.0 (20)
HuatuoGPT	10.0 (3)	20.0 (6)	0.60	5.0 (3)	13.3 (8)	0.68	3.0 (6)	7.0 (14)
Human								
Medical Student	3.3 (1)	—	—	3.3 (2)	—	—	6.0 (12)	—
Senior Physician	40.0 (12)	—	—	35.5 (21)	—	—	15.0 (30)	—

5.2 THE GAP TO HUMAN EXPERTISE: A SOBERING REALITY

To provide a crucial, real-world anchor for model performance, we benchmarked leading VLMs against both the ideal Ground Truth (expert consensus) and realistic human baselines. The results, visualized in Figure 4(Left), reveal a sobering chasm. On Direct Diagnosis tasks, the top-performing VLM, MedGemma, reached 30.0% pass@1 accuracy, falling 10 percentage points short of the Senior Physician’s 40.0% and barely surpassing a Medical Student. This performance gap widens dramatically in the *Complex Diseases* subset, where the Senior Physician’s performance (35.5%) is nearly double that of MedGemma (18.3%). This quantitative and clinically meaningful gap validates our benchmark’s difficulty and underscores the immense distance to human-level clinical competence.

5.3 WHY DO MODELS FAIL? A SYSTEMATIC ERROR ANALYSIS

To diagnose the root cause of this performance gap, we performed a systematic analysis of 100 incorrect model responses. The distribution of primary error types (Figure 4(Right)) reveals that the primary bottleneck for current VLMs is not perception, but reasoning. A striking 51% of failures were classified as Reasoning Failures, where models correctly identified key findings but failed to synthesize them into a correct diagnosis. This rate is nearly double that of Perceptual Failures (27%). This key finding allows us to define the “lower bound” of current VLM capabilities. Our results suggest this capability floor is set not by a lack of perceptual acuity, but by a fundamental deficit in integrative clinical reasoning. This directly explains the observed disconnect between high linguistic fluency and low diagnostic accuracy, highlighting the necessity of Depth-Axis benchmarks for diagnosing and ultimately fixing these core reasoning deficiencies.

5.4 ADDITIONAL FINDINGS

Foundation Models vs. Medical-Specialized Models. Our results reveal a nuanced relationship between generalist and specialist VLMs. On single-best-guess accuracy (pass@1), the medical-specialized MedGemma-27B-it is the clear leader, demonstrating the value of domain-specific fine-tuning for diagnostic precision. However, on differential diagnosis generation (pass@5), large generalist models like Gemini 2.5-Flash retain an edge, likely due to their broader generative

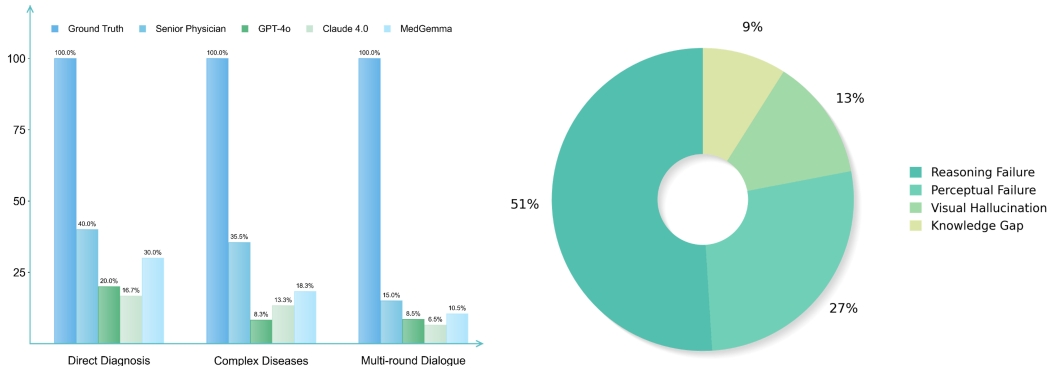


Figure 4: **The Performance Gap to Human Expertise and a Systematic Diagnosis of Model Failures.** (Left) A direct comparison of pass@1 accuracy. The "Ground Truth" represents the expert consensus answer. The "Senior Physician" bar shows the performance of a board-certified neurologist in a blinded test, providing a realistic human expert baseline. All evaluated VLMs perform significantly below this realistic baseline, widening the gap as task complexity increases. (Right) Distribution of primary error types from a systematic analysis of incorrect model responses. Reasoning Failure is the dominant cause of error, suggesting the primary bottleneck is cognitive, not perceptual.

capabilities. This suggests that optimal clinical AI may require a synthesis of both deep specialization and generative breadth.

Evaluation Efficiency. As a Depth-Axis benchmark, *Neural-MedBench* is deliberately designed for high signal-to-noise ratio and evaluation efficiency. Our diagnostic prompts are carefully engineered to elicit rich, multi-faceted reasoning from a compact set of cases. As summarized in Table 3, this high-density design reduces inference token costs by over an order of magnitude (10x) compared to large-scale Breadth-Axis benchmarks like *OmniMed-VQA*, while maintaining high diagnostic difficulty. This cost-effectiveness is a key feature, as it lowers the barrier for academic labs and enables practical, multi-sample robustness analyses (e.g., via temperature sweeps), which are often computationally prohibitive on larger datasets but are essential for assessing model reliability.

Table 3: GPT-4o performance on different benchmarks

Benchmark	Number of Images	Cost of Image Tokens	Passing Rate (%)
GMAI-MMBench	12K	\$30.00	53.96
OmniMed-VQA	128K	\$320.00	29.74
Neural-MedBench	1K	\$2.50	9.67

6 CONCLUSION

In this work, we challenged the prevailing paradigm of evaluating medical VLMs through the lens of classification accuracy. We argued that this approach creates an "evaluation illusion," and proposed a more complete Two-Axis Framework that mandates complementary assessment of both Breadth (statistical generalization) and Depth (reasoning fidelity). To operationalize this missing Depth axis, we introduced *Neural-MedBench*, a compact, diagnostically complex benchmark for clinical neurology. Our extensive experiments yielded a sobering conclusion: a model’s success on large-scale, Breadth-Axis benchmarks is a poor predictor of its ability to perform deep clinical reasoning. We found that even state-of-the-art models are consistently outperformed by human clinicians and that their failures stem primarily from fundamental breakdowns in reasoning, not perception.

While *Neural-MedBench* provides a crucial new perspective, we acknowledge its limitations. Its intentionally compact scale restricts broad statistical claims, and its current focus is on diagnostic

reasoning rather than the full clinical workflow. The sample size for our human baseline, while offering vital insights, is also modest. These limitations, however, illuminate a clear and exciting roadmap for future work. The next generation of Depth-Axis benchmarks must expand in both scale and clinical scope, incorporating more diverse and underrepresented conditions, longitudinal data, and multi-center variability to systematically study domain shift. Notably, *Neural-MedBench* is designed as a continually evolving resource: the present set of cases and tasks reflects the state at submission, and its scale and coverage will be continuously extended.

Ultimately, *Neural-MedBench* is more than a dataset; it is a diagnostic tool for the field itself, providing a reproducible methodology to probe the core reasoning capabilities of our most advanced models. By offering this high-resolution lens and committing to its ongoing evolution, we aim to shift the community’s focus from a narrow pursuit of accuracy towards the development of AI systems that possess genuine, trustworthy clinical reasoning. This benchmark serves as a foundational step in that critical journey.

7 ETHICS DETAILS

Data used in this study were obtained from the Alzheimer’s Disease Neuroimaging Initiative (ADNI) database (adni.loni.usc.edu), the OASIS dataset, Radiopaedia, and case reports from articles published in *The Journal of the American Medical Association (JAMA)*. All data were accessed with prior approval and are fully de-identified.

- **ADNI:** Investigators within ADNI contributed to data collection but did not participate in the analysis or writing of this manuscript. A comprehensive list of ADNI investigators is available at: [ADNI Acknowledgement List](#). Data collection and sharing for ADNI were funded by the National Institute on Aging (U01 AG024904), the Department of Defense (W81XWH-12-2-0012), and other sponsors listed on the ADNI website. This manuscript was reviewed by the ADNI Data and Publications Committee prior to submission.
- **OASIS:** A portion of the OASIS dataset was restructured to comply with privacy protection protocols, ensuring that no personally identifiable information was included. Throughout the process, we adhered strictly to OASIS’s privacy guidelines, safeguarding participant confidentiality.
- **Radiopaedia:** Radiopaedia data used in this study are provided under the Creative Commons Attribution-NonCommercial-ShareAlike 3.0 (CC-BY-NC-SA 3.0) license. The data were utilized for non-commercial purposes with proper attribution to Radiopaedia and are redistributed under the same licensing terms.

8 REPRODUCIBILITY STATEMENT

All experiments in this study are based on our *Neural-MedBench* dataset. Its sources, filtering, and construction process are described in Appendix A. The full dataset is publicly available on Hugging Face at <https://huggingface.co/datasets/Reisen301/Neural-MedBench> for reuse and verification.

REFERENCES

- Anthropic. Claude haiku, 2024. URL <https://www.anthropic.com>.
- Jinze Bai, Shuai Bai, Shusheng Yang, Shijie Wang, Sinan Tan, Peng Wang, Junyang Lin, Chang Zhou, and Jingren Zhou. Qwen-vl: A versatile vision-language model for understanding, localization, text reading, and beyond. *arXiv preprint arXiv:2308.12966*, 2023. URL <https://arxiv.org/abs/2308.12966>.
- Patrick Bilic, Patrick F Christ, Eugene Vorontsov, Grzegorz Chlebus, Hao Chen, Qi Dou, Chi-Wing Fu, Xu Han, Pheng-Ann Heng, Jürgen Hesser, et al. The liver tumor segmentation benchmark (lits). *arXiv preprint arXiv:1901.04056*, 2019.
- Gheorghe Comanici, Eric Bieber, Mike Schaekermann, Ice Pasupat, Noveen Sachdeva, Inderjit Dhillon, Marcel Blistein, Ori Ram, Dan Zhang, Evan Rosen, et al. Gemini 2.5: Pushing the frontier

- with advanced reasoning, multimodality, long context, and next generation agentic capabilities. *arXiv preprint arXiv:2507.06261*, 2025.
- Jadon Geathers, Yann Hicke, Colleen Chan, Niroop Rajashekar, Sarah Young, Justin Sewell, Susannah Cornes, Rene F Kizilcec, and Dennis Shung. Benchmarking generative ai for scoring medical student interviews in objective structured clinical examinations (osces). In *International Conference on Artificial Intelligence in Education*, pp. 231–245. Springer, 2025.
- Maxime Griot, Coralie Hemptinne, Jean Vanderdonckt, and Demet Yuksel. Large language models lack essential metacognition for reliable medical reasoning. *Nature communications*, 16(1):642, 2025.
- Zexuan He, Yifan Peng, Le Lu, Xiaosong Wang, and Ronald M Summers. Pathvqa: 30000+ questions for medical visual question answering. *arXiv preprint arXiv:2003.10286*, 2020.
- Jack Hessel, Ari Holtzman, Maxwell Forbes, Ronan Le Bras, and Yejin Choi. Clipscore: A reference-free evaluation metric for image captioning. *arXiv preprint arXiv:2104.08718*, 2021.
- Yutao Hu, Tianbin Li, Quanfeng Lu, Wenqi Shao, Junjun He, Yu Qiao, and Ping Luo. Omnimed-vqa: A new large-scale comprehensive evaluation benchmark for medical lvlm. *arXiv preprint arXiv:2402.09181*, 2024.
- Jeremy Irvin, Pranav Rajpurkar, Michael Ko, Yifan Yu, Silvana Ciurea-Ilcus, Chris Chute, Henrik Marklund, Behzad Haghighi, Robyn Ball, Katie Shpanskaya, et al. Chexpert: A large chest radiograph dataset with uncertainty labels and expert comparison. *Proceedings of the AAAI Conference on Artificial Intelligence*, 33(01):590–597, 2019.
- Saahil Jain, Ashwin Agrawal, Adriel Saporta, Steven Q H Truong, Du Nguyen Duong, Tan Bui, Pierre Chambon, Yuhao Zhang, Matthew P Lungren, Andrew Y Ng, et al. Radgraph: Extracting clinical entities and relations from radiology reports. *arXiv preprint arXiv:2106.14463*, 2021.
- Alistair E W Johnson, Tom J Pollard, Seth J Berkowitz, Nathaniel R Greenbaum, Matthew P Lungren, Chih-ying Deng, Roger G Mark, and Steven Horng. Mimic-cxr, a de-identified publicly available database of chest radiographs with free-text reports. *Scientific Data*, 6(1):317, 2019.
- Tzu-Lin Kuo, Feng-Ting Liao, Mu-Wei Hsieh, Fu-Chieh Chang, Po-Chun Hsu, and Da-Shan Shiu. Rad-bench: Evaluating large language models capabilities in retrieval augmented dialogues. *arXiv preprint arXiv:2409.12558*, 2024.
- Jason J Lau, Soumya Gayen, Asma Ben Abacha, and Dina Demner-Fushman. A dataset of clinically generated visual questions and answers about radiology images. *Scientific data*, 5(1):1–10, 2018.
- Chunyu Li, Cliff Wong, Sheng Zhang, Naoto Usuyama, Haotian Liu, Jianwei Yang, Tristan Naumann, Hoifung Poon, and Jianfeng Gao. Llava-med: Training a large language-and-vision assistant for biomedicine in one day. In *NeurIPS 23 Datasets & Benchmarks Track (Spotlight)*, 2023. URL <https://github.com/microsoft/LLaVA-Med>.
- Bjoern H Menze, Andras Jakab, Stefan Bauer, Jayashree Kalpathy-Cramer, Keyvan Farahani, Justin Kirby, Yuliya Burren, Nils Porz, Johannes Slotboom, Roland Wiest, et al. The multimodal brain tumor image segmentation benchmark (brats). *IEEE Transactions on Medical Imaging*, 34(10):1993–2024, 2015.
- Michael Moor, Qian Huang, Shirley Wu, Michihiro Yasunaga, Cyril Zakka, Yash Dalmia, Eduardo Pontes Reis, Pranav Rajpurkar, and Jure Leskovec. Med-flamingo: a multimodal medical few-shot learner. In Stefan Heggelmann, Antonio Parziale, Divya Shanmugam, Shengpu Tang, Mercy Nyamewaa Asiedu, Serina Chang, Tom Hartvigsen, and Harvaneet Singh (eds.), *Proceedings of the 3rd Machine Learning for Health Symposium*, volume 225 of *Proceedings of Machine Learning Research*, pp. 353–367. PMLR, 10 Dec 2023. URL <https://proceedings.mlr.press/v225/moor23a.html>.
- OpenAI. Gpt-4o system card, 2024. URL <https://arxiv.org/abs/2410.21276>.

- Johannes Rückert, Louise Bloch, Raphael Brüngel, Ahmad Idrissi-Yaghir, Henning Schäfer, Cynthia S Schmidt, Sven Koitka, Obioma Pelka, Asma Ben Abacha, Alba G. Seco de Herrera, et al. Rocov2: Radiology objects in context version 2, an updated multimodal image dataset. *Scientific Data*, 11(1):688, 2024.
- Richard M Schwartzstein. Clinical reasoning and artificial intelligence: can ai really think? *Transactions of the American Clinical and Climatological Association*, 134:133, 2024.
- Andrew Sellergren, Sahar Kazemzadeh, Tiam Jaroensri, Atilla Kiraly, Madeleine Traverse, Timo Kohlberger, Shawn Xu, Fayaz Jamil, Cían Hughes, Charles Lau, et al. Medgemma technical report. *arXiv preprint arXiv:2507.05201*, 2025.
- Ramprasaath R Selvaraju, Michael Cogswell, Abhishek Das, Ramakrishna Vedantam, Devi Parikh, and Dhruv Batra. Grad-cam: visual explanations from deep networks via gradient-based localization. *International journal of computer vision*, 128:336–359, 2020.
- Arnaud A A Setio, Andrea Traverso, Timo de Bel, Max S Berens, Chris van den Bogaard, Piergiorgio Cerello, Hoo-Chang Chen, Qi Dou, Maria E Fantacci, Pierre Geurts, et al. Validation, comparison, and combination of algorithms for automatic detection of pulmonary nodules in computed tomography images: the luna16 challenge. *Medical Image Analysis*, 42:1–13, 2017.
- Jeffrey Siegelman, Lisa Bernstein, Jennifer Goedken, Linda Lewin, Jason Schneider, Martha Ward, and Hugh Stoddard. Assessment of clinical reasoning during a high stakes medical student osce. *Perspectives on Medical Education*, 13(1):629, 2024.
- Akshay Smit, Saahil Jain, Pranav Rajpurkar, Anuj Pareek, Andrew Y Ng, and Matthew P Lungren. Chexbert: combining automatic labelers and expert annotations for accurate radiology report labeling using bert. *arXiv preprint arXiv:2004.09167*, 2020.
- J. Smith et al. Expert-of-experts verification and alignment (eval): Clinician-augmented evaluation of large language models in gastrointestinal bleeding. *NPJ Digital Medicine*, 8(1):1589, 2025.
- Xiangru Tang, Daniel Shao, Jiwoong Sohn, Jiapeng Chen, Jiayi Zhang, Jinyu Xiang, Fang Wu, Yilun Zhao, Chenglin Wu, Wenqi Shi, et al. Medagentsbench: Benchmarking thinking models and agent frameworks for complex medical reasoning. *arXiv preprint arXiv:2503.07459*, 2025.
- Doubao Team. The doubao visual language model officially released with general model capability fully comparable to gpt-4o, 2024. URL <https://team.doubao.com/>.
- Xiaosong Wang, Yifan Peng, Le Lu, Zhiyong Lu, Mohammadhadi Bagheri, and Ronald M Summers. Chestx-ray8: Hospital-scale chest x-ray database and benchmarks on weakly-supervised classification and localization of common thorax diseases. *Proceedings of the IEEE Conference on Computer Vision and Pattern Recognition (CVPR)*, 2017.
- Stefan Winzeck, Ali Hakim, Richard McKinley, Joana Pinto, Victor Alves, Carlos Silva, Mauricio Reyes, Alessandro Crimi, Bjoern Menze, Daniel Rueckert, et al. Isles 2015—a public evaluation benchmark for ischemic stroke lesion segmentation from multispectral mri. *Medical Image Analysis*, 35:250–269, 2017.
- Chaoyi Wu, Xiaoman Zhang, Ya Zhang, Yanfeng Wang, and Weidi Xie. Towards generalist foundation model for radiology by leveraging web-scale 2d&3d medical data. *arXiv preprint arXiv:2308.02463*, 2023. URL <https://arxiv.org/abs/2308.02463>.
- Jiancheng Yang, Rui Shi, Donglai Wei, Zequan Liu, Lin Zhao, Bilian Ke, Hanspeter Pfister, and Bingbing Ni. Medmnist v2-a large-scale lightweight benchmark for 2d and 3d biomedical image classification. *Scientific Data*, 10(1):41, 2023.
- Tianyi Zhang, Varsha Kishore, Felix Wu, Kilian Q Weinberger, and Yoav Artzi. Bertscore: Evaluating text generation with bert. *arXiv preprint arXiv:1904.09675*, 2019.
- Y. Zhang et al. Llmeval-med: Benchmarking large language models for clinical evaluation with expert-designed scenarios. *arXiv preprint arXiv:2506.04078*, 2025.

- Yuxuan Zhang, Yifan Wang, Ya Zhang, Yanfeng Wang, and Liang He. Medfmc: A real-world dataset and benchmark for foundation model adaptation in medical image classification. *Scientific Data*, 10(1):1–11, 2023.
- Weihai Zhi, Jiayan Guo, and Shangyang Li. Medgr²: Breaking the data barrier for medical reasoning via generative reward learning. *arXiv preprint arXiv:2508.20549*, 2025.
- Yuxuan Zhou, Xien Liu, Chen Ning, and Ji Wu. Multifaceteval: Multifaceted evaluation to probe llms in mastering medical knowledge. *arXiv preprint arXiv:2406.02919*, 2024.
- Yakun Zhu, Zhongzhen Huang, Linjie Mu, Yutong Huang, Wei Nie, Jiaji Liu, Shaoting Zhang, Pengfei Liu, and Xiaofan Zhang. Diagnosisarena: Benchmarking diagnostic reasoning for large language models. *arXiv preprint arXiv:2505.14107*, 2025.

A ADDITIONAL DATASET DETAILS

Data Source Breakdown. To ensure transparency and reproducibility, we provide a detailed overview of the composition of *Neural-MedBench*. As shown in Table 4, the benchmark draws on four carefully vetted sources spanning public neuroimaging cohorts, curated online repositories, and peer-reviewed clinical case reports. Together these sources yield a heterogeneous pool of conditions ranging from common neurodegenerative diseases to rare atypical presentations, enabling a broad coverage of diagnostic challenges.

Table 4: Proportional breakdown of all cases in *Neural-MedBench* by source.

Source	Proportion of Cases (%)	Primary Conditions Covered
ADNI	18.2	Alzheimer’s Disease, Mild Cognitive Impairment
OASIS	9.1	Alzheimer’s Disease, Normal Aging
Radiopaedia	45.5	Stroke, CNS Infections, Autoimmune Encephalitis, Tumors
JAMA Neurology	36.4	Rare Diseases, Atypical Presentations

Case Curation Protocol. As illustrated in Figure 5, the construction of *Neural-MedBench* followed a rigorous, four-stage, funnel-shaped pipeline to distill an initial pool of over 2,000 candidate cases into the final 120 high-density cases. The stages were:

- Pooling and Filtering:** We first pooled cases from our sources and filtered them to retain only those with sufficient multimodal completeness (e.g., clear imaging, patient history, and clinical notes).
- Expert Curation:** A panel of senior neurologists reviewed the filtered cases for clinical plausibility, diagnostic complexity, and educational value, selecting for scenarios that require deep reasoning.
- Annotation of Ground Truth:** For each selected case, the expert panel systematically annotated the ground truth, which includes not only the final diagnosis but also differential diagnoses, key lesion characteristics, and the full explanatory reasoning chain.
- Consensus Review and Challenge Validation:** Finally, all annotated cases underwent a consensus review to resolve any disagreements. In this stage, we also performed a challenge validation using baseline models to filter out diagnostically trivial cases and ensure every case in the final benchmark presents a meaningful reasoning challenge.

This multi-stage process ensures that each of the 120 cases is diagnostically rich, clinically authentic, and serves as a potent test of a model’s reasoning capabilities.

Distribution of Clinical Conditions and Reasoning Tasks. Figure 6 provides a dual view of the benchmark’s diversity. The top panel (sunburst chart) illustrates the hierarchical distribution of the 120 clinical cases across a wide spectrum of neurological diseases. It demonstrates a balanced coverage of both common conditions like Alzheimer’s disease and a long tail of rare or diagnostically challenging

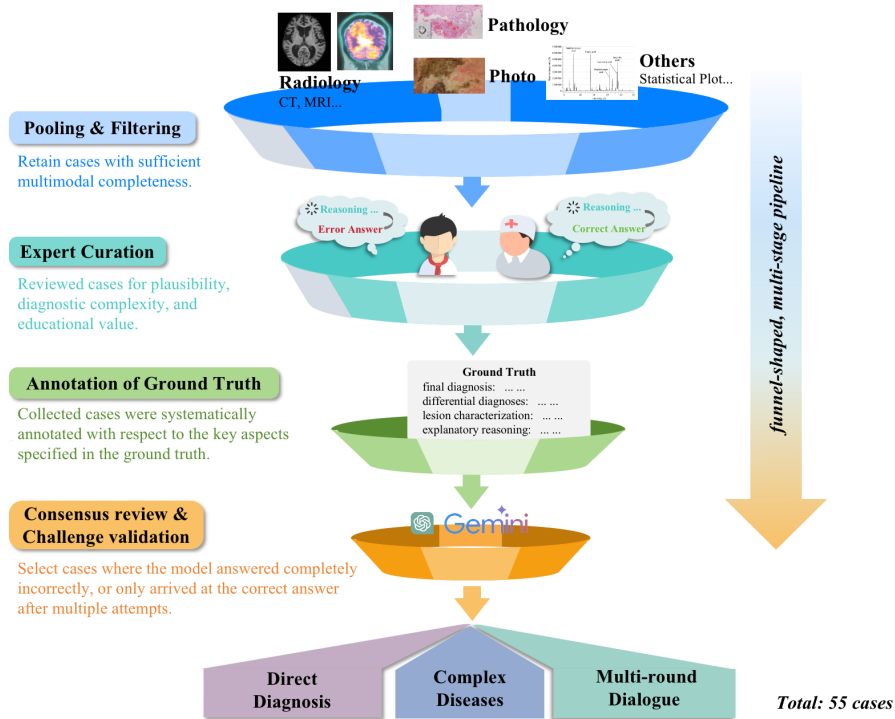


Figure 5: **The four-stage, funnel-shaped curation pipeline for Neural-MedBench.** The process distills over 2,000 initial candidates into 120 final cases by systematically filtering for multimodal completeness, curating for diagnostic complexity, annotating a rich ground truth, and validating the final reasoning challenge.

disorders (e.g., PERM, PAVF), ensuring a robust test of model generalization beyond frequency bias. The bottom panel details the distribution of the 200 questions across the three core cognitive capabilities probed by our benchmark: Differential Diagnosis (29%), Lesion Recognition (25%), and Rationale Generation (46%). The benchmark is thus heavily weighted towards higher-order reasoning, moving far beyond simple recognition.

Content Statistics. Figure 7 presents the detailed distributions of token counts and image sizes for the dataset. Panel (a) shows the distribution of English token counts in the clinical narratives, confirming that while we controlled for extreme length variations, a natural diversity remains. Panel (b) illustrates the variability in total image pixels per case, reflecting the real-world heterogeneity in MRI/CT acquisition protocols (e.g., number of sequences and slices). These statistics underscore that Neural-MedBench preserves authentic data characteristics while maintaining a balanced design for fair evaluation.

Limitations of Dataset Composition. While Neural-MedBench was deliberately curated for diagnostic depth, we acknowledge several limitations in its current composition. First, the total number of tasks (200) is modest, reflecting a deliberate trade-off for the high-density, expert-intensive annotation required for reasoning evaluation. Second, the distribution of conditions is biased toward disorders with pronounced imaging correlates (e.g., stroke, tumors), with less representation of disorders that are primarily functional or metabolic. Third, although cases are drawn from multiple sources, the benchmark does not yet systematically capture the full spectrum of domain shift across hospitals, scanners, or reporting conventions. Finally, the current release represents only an initial

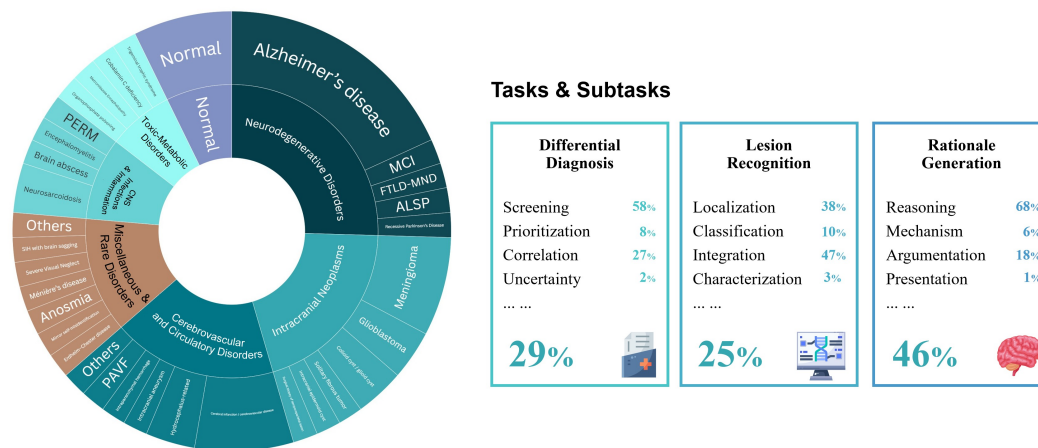


Figure 6: **Hierarchical Distribution of Neurological Diseases and Reasoning Tasks in Neural-MedBench.** (Top) The sunburst chart illustrates the distribution of the all clinical cases across a wide range of neurological conditions, from high-level categories (e.g., Neurodegenerative Disorders, Intracranial Neoplasms) to specific diagnoses (e.g., Alzheimer’s disease, Glioblastoma), including a significant proportion of rare and complex disorders. (Bottom) The task distribution across the 200 questions, categorized into three core reasoning families: Differential Diagnosis (29%), Lesion Recognition (25%), and Rationale Generation (46%). Each family is further broken down into specific cognitive subtasks.

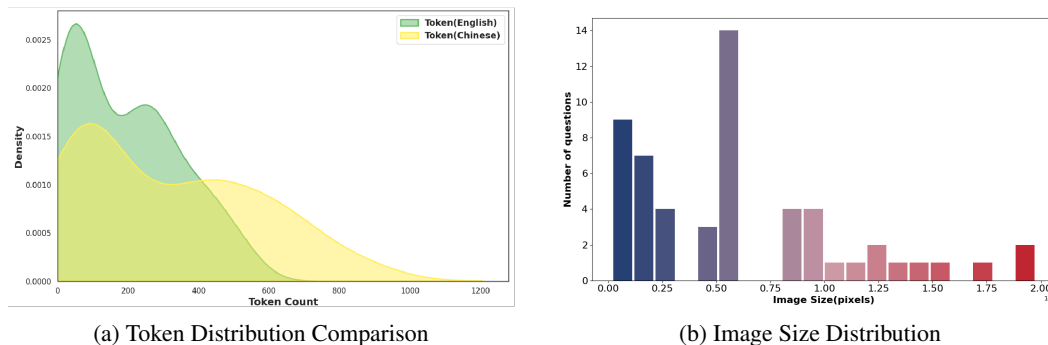


Figure 7: **Detailed content statistics for Neural-MedBench.**

stage of the benchmark, which will be progressively expanded over time. These considerations underscore that Neural-MedBench is best interpreted as a high-resolution stress test for reasoning fidelity, not a comprehensive benchmark for statistical generalization. To address these limitations, future iterations will continuously grow in both scale and disease spectrum, with particular emphasis on underrepresented conditions, longitudinal follow-up, and multi-center variability, ensuring that the benchmark remains a continually evolving resource for the community.

B PROMPT TEMPLATES

We employed a structured role-prompting strategy to ensure that model behavior adhered to clinical logic.

”You are an experienced neurology expert, skilled in analyzing complex cases and providing preliminary diagnoses based on a combination of medical imaging and clinical descriptions. Please carefully answer the following questions based on the provided information.”

Example Task Prompt.

Patient history: 47-year-old female with progressive motor weakness and intermittent visual disturbances.

Imaging: Multi-sequence MRI (T2, FLAIR) uploaded below.

Task: Please provide your most likely diagnosis, differential diagnoses, and explain your reasoning.

All multimodal inputs were interleaved with text. Imaging data were encoded in base64 and inserted as `<image>` tokens when supported by the model.

We employed a baseline model as an automatic judge to assess the agreement between the model’s outputs and the reference answers. The evaluation is conducted using a fixed prompt.

You are an expert medical evaluator judging the accuracy of AI-generated diagnoses against reference answers.

*model_answer: [model_answer]
ref_answer: [ref_answer]*

Guidelines:

- 1. The model’s diagnosis is correct if it captures the main pathology/condition mentioned in the reference diagnosis.*
- 2. Minor differences in terminology or additional details provided by the model are acceptable as long as the core diagnosis is correct.*
- 3. If the reference diagnosis contains multiple conditions, the model should identify at least the primary condition to be considered correct.*
- 4. Ignore differences in formatting, grammar, or level of detail if the core diagnosis is correct.*

Please provide a direct answer at the beginning, [yes] or [no].

C MODEL CONFIGURATIONS AND HYPERPARAMETERS

To ensure reproducibility, we list the exact model versions evaluated:

- GPT-4o: gpt-4o-2025-03-26
- Gemini 2.5-Flash: gemini-2.5-flash-preview-04-17
- Gemini 2.0-Flash: gemini-2.0-flash-exp
- Claude 4.0 Sonnet: claude-sonnet-4-20250514
- Claude 3.7 Sonnet: claude-3-7-sonnet-20250219
- Claude 3.5 Sonnet: claude-3-5-sonnet-20241022
- Qwen-VL-2.5: qwen-vl-2.5-32b
- Doubao: doubao-1.5-vision-pro-32k-250115
- LLaVA-Med: llava-med-v1.5-mistral-7b
- RadFM: chaoyi-wu/RadFM
- Med-Flamingo: snap-stanford/med-flamingo
- Huatuo-GPT-Vision: huatuo-gpt-vision-7b
- MedGemma: MedGemma-27B-it

C.1 HYPERPARAMETERS

Table 5 summarizes the key hyperparameter settings used across all experiments. For diagnostic accuracy (pass@1, pass@5), predictions were generated with nucleus sampling ($p = 0.95$, $T = 0.7$). For text similarity evaluation, we used BERTScore with `roberta-large`. All confidence intervals are reported using the Wilson score interval.

Table 5: Decoding hyperparameters used for each model

Model	Hyperparameters
GPT-4o	temperature=0.7, top_p=0.95, seed=22
Gemini 2.5-Flash	temperature=0.7, top_p=0.95
Gemini 2.0-Flash	temperature=0.7, top_p=0.95
Claude 4 Sonnet	temperature=0.7, top_p=0.95
Claude 3.7 Sonnet	temperature=0.7, top_p=0.95
Claude 3.5 Sonnet	temperature=0.7, top_p=0.95
Qwen-VL-2.5	temperature=0.7, top_p=0.95
DouBao	temperature=0.7, top_p=0.95
LLaVA-Med	temperature=0.7, top_p=0.95
MedGemma	temperature=0.7, top_p=0.95
RadFM	temperature=0.7, top_p=0.95
Med-Flamingo	temperature=0.7, top_p=0.95
HuatuogPT	temperature=0.7, top_p=0.95

D CONFIDENCE INTERVALS

For diagnostic accuracy metrics, we report 95% confidence intervals using the Wilson score interval:

$$CI = \frac{1}{1 + \frac{z^2}{n}} \left(\hat{p} + \frac{z^2}{2n} \pm z \sqrt{\frac{\hat{p}(1 - \hat{p})}{n} + \frac{z^2}{4n^2}} \right) \quad (1)$$

where \hat{p} is observed accuracy, n is sample size, and $z = 1.96$ for 95% confidence.

E GRADER BIAS CONSIDERATIONS

A potential concern arises from the use of GPT-4o both as a benchmarked model and as the primary LLM-based grader. To mitigate self-evaluation bias, we conducted a rigorous clinician-in-the-loop calibration, finding a very high correlation with expert consensus scores (Pearson’s $r > 0.9$). Importantly, no systematic advantage was observed for GPT-4o outputs compared to other models under the same rubric. In addition, our evaluation protocol is hybridized with semantic similarity metrics (BERTScore) and direct clinician validation, ensuring that grading robustness does not rely solely on GPT-4o. For future iterations, we plan to expand the grader pool by incorporating multiple LLMs (e.g., Claude, Gemini) and additional clinician review to further enhance fairness and reproducibility.

F ERROR TAXONOMY ANNOTATION PROTOCOL

To better understand failure modes, two board-certified neurologists independently annotated 100 randomly sampled incorrect responses using the following taxonomy:

- **Reasoning Failure:** Correctly observed features but incorrect causal inference.
- **Perceptual Failure:** Misinterpretation of visual features (e.g., lesion missed).
- **Visual Hallucination:** Fabricated findings not present in the input data.
- **Knowledge Gap:** Missing medical knowledge required for correct diagnosis.

Across the incorrectly answered cases, the distribution of primary error types was: Reasoning Failure 51%, Perceptual Failure 27%, Visual Hallucination 13%, and Knowledge Gap 9%. These proportions suggest that current multimodal language–vision systems for neuroimaging are limited more by inference and decision-making than by raw visual recognition or encyclopedic recall.

Disagreements were resolved by consensus. Inter-rater agreement was $\kappa = 0.82$, indicating strong consistency.

Reasoning Failure (51%). The dominant failure mode reflects cases in which salient image findings were noted but mapped to an incorrect diagnosis or pathophysiologic explanation. Typical patterns included misweighting across MRI sequences (e.g., over-interpreting FLAIR hyperintensity without integrating diffusion restriction), conflating acute and chronic stigmata, and collapsing multi-lesion presentations into a single etiology. These errors point to gaps in causal and temporal modeling—models can “see” but struggle to structure evidence, adjudicate competing hypotheses, or apply exclusion criteria.

Perceptual Failure (27%). Pure detection/characterization mistakes were the next largest category. Contributing factors included low signal-to-noise, motion artifact, and small lesion size.

Visual Hallucination (13%). In nearly one-fifth of failures, the model asserted findings that were not present (e.g., “midline shift,” “ring-enhancing lesion”) and then built a diagnosis on those fictitious observations. This is a distinct safety risk because it couples perceptual fabrication with persuasive language.

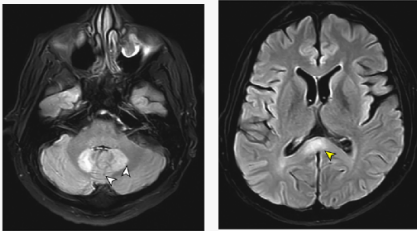
Knowledge Gap (9%). Pure deficits in medical knowledge were least common. Notably, the relatively small share here underscores that, for common entities, the models “know enough” but still reason unreliably.

G ERROR CASES

To provide a more granular and intuitive understanding of the failure modes quantified in our main analysis, this section presents a series of representative error cases from *Neural-MedBench*. Figure 8 presents a Level 2 complex diagnosis task. This task specifically tests the model’s ability to link a pharmacological history to specific neuroimaging findings, a common real-world clinical challenge. The subsequent pages display 14 additional failure cases, presented in groups of figure (Figure 9 to Figure 12). Together, these qualitative examples provide concrete evidence for the limitations of current VLMs and highlight the critical importance of Depth-Axis evaluation.

Level 2 Error Case

A 41-year-old quadriplegic male patient, who had been bedridden for 12 years due to a traffic accident, had multiple bedsores and had been applying metronidazole powder (with gel) to the bedsores for the past 8 to 10 months. She presented to the emergency room of our hospital with complaints of slurred speech and facial tilting for 2 days, accompanied by a seizure. She had a history of type 2 diabetes mellitus. Physical examination: The patient was conscious, oriented, had slurred speech, could follow simple instructions, and had no signs of meningeal irritation. His pulse rate was 101 beats per minute and blood pressure was 120/80 mmHg.



Q: Combine the patient's medical records and pictures to analyze and diagnose the most likely disease?

Reference & Model Answers

<p>★ <i>Ground truth</i></p> <p><i>Metronidazole toxicity-induced encephalopathy</i></p>	 <p><i>Central Pontine Myelinolysis</i></p> <p>✗ Reasoning Failure</p>	 <p><i>Metabolic Encephalopathies</i></p> <p>✗ Knowledge Gap</p>	 <p><i>Acute Ischemic Stroke</i></p> <p>✗ Reasoning Failure</p>
--	---	---	--

Figure 8: A representative Level 2 failure case demonstrating both Reasoning Failure and Knowledge Gap.

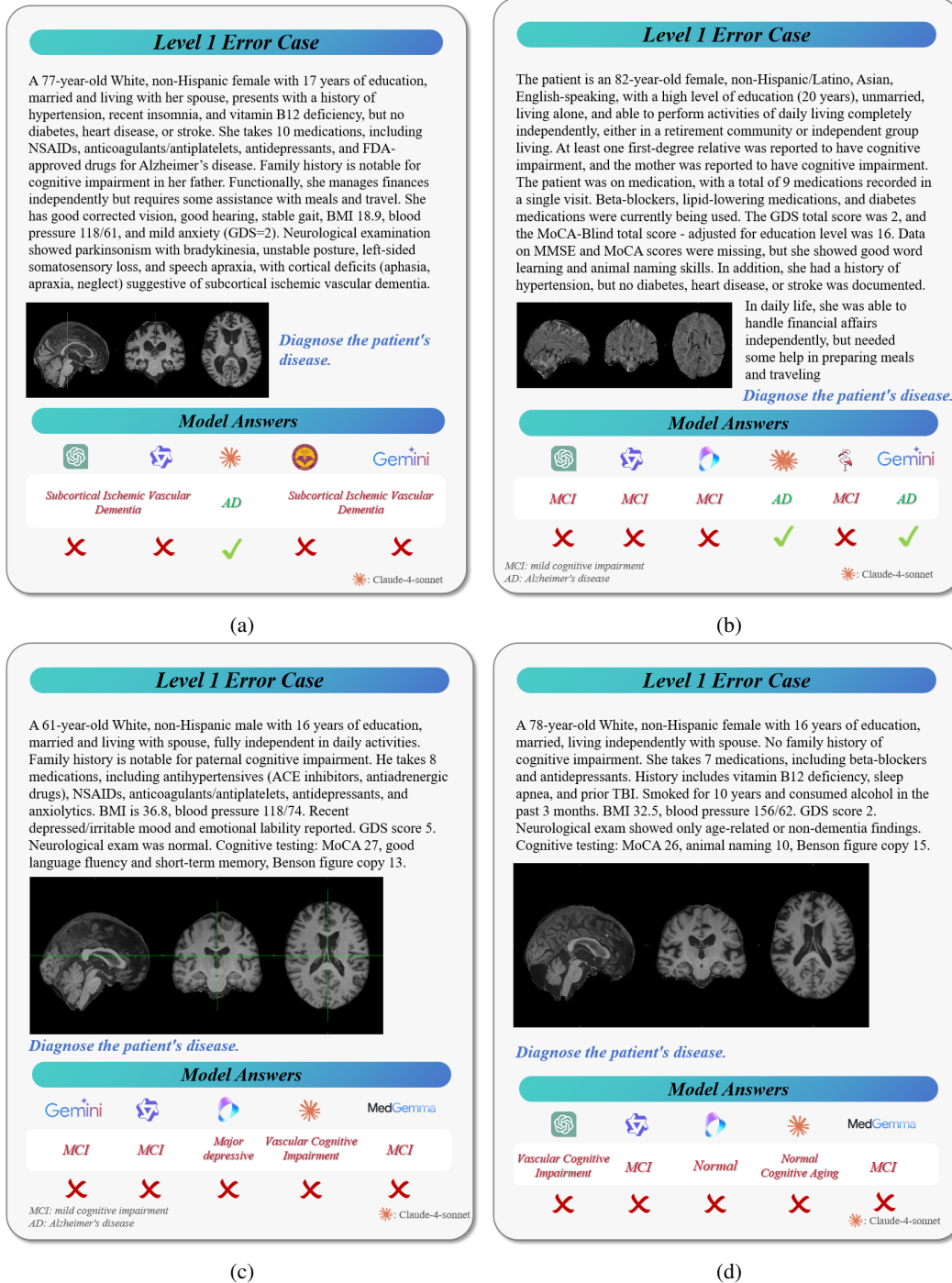
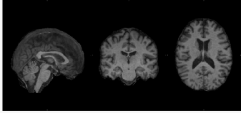


Figure 9: Additional error cases.

Level 1 Error Case

The patient is a 20-year-old female, right-handed. Specific information about her educational background and socioeconomic status is currently lacking. Due to the missing MMSE and CDR scores, her current cognitive function and dementia status cannot be directly assessed. Imaging data showed that her estimated total intracranial volume was 1749 cubic centimeters and the standardized whole brain volume was 0.84, which was within the normal range, indicating that her brain structure was not significantly abnormal in volume. The intracranial artery score was 1.441, suggesting that there may be certain cerebrovascular health problems, but the specific impact needs further evaluation. Due to the missing results of the delayed recall test, it is impossible to fully understand her long-term memory ability.



Diagnose the patient's disease.

Model Answers

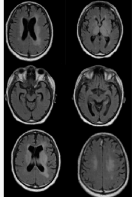
Cerebrovascular issues	?	Normal	Cerebrovascular issues	Cerebrovascular issues
✗	✗	✓	✗	✗

(a)

Level 3 Error Case

Presentation: Acute headache and impaired consciousness
Neurological exam: non-focal
Age: 50 years
Gender: Male

Q1: What abnormality is indicated by the increased density within the deep cerebral veins on non-contrast CT?
Q2: What is the likely cause of bilateral thalamic and basal ganglia hypoattenuation observed on CT?
Q3: What is the significance of the absence of normal flow signal in the deep cerebral veins on MRV?
Q4: How do bilateral thalamic hemorrhages seen on SWI contribute to the diagnosis?
Q5: What vascular structures are most likely involved given the pattern of abnormalities on imaging?



Reference & Model Answers

✦ Ground truth		
✦ Deep cerebral vein thrombosis	Venous Thrombosis	Deep cerebral vein thrombosis
✦ Venous congestion edema	Hypoxic-Ischemic encephalopathy	Bilateral deep gray infarction
✦ Venous occlusion on MRV	Deep cerebral venous thrombosis	Venous flow signal absent
✦ Bilateral thalamic hemorrhage	Venous thrombosis or hypertension	Bilateral thalamic hemorrhages
✦ Internal cerebral vein thrombosis	Internal cerebral veins	Middle and anterior cerebral arteries

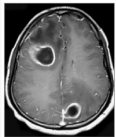
*Core diagnostic results extracted from the diagnostic text generated by the model

(b)

Level 2 Error Case

A 34-year-old man presented with a 1-month history of headache, diplopia, seizures, and altered consciousness for 1 week. The patient had had 2 seizures characterized by a tonic left deviation of the head and eyeballs, followed by brief tonic-clonic activity of the extremities, and confusion lasting 10 to 15 minutes after the seizure. The patient denied a history of fever, head trauma, limb weakness, or vomiting. The patient was a vegetarian and did not smoke or drink alcohol. The patient denied a history of drug addiction. Physical examination revealed that the patient was confused ... Liver and kidney function tests were normal. HIV enzyme-linked immunosorbent assay was unreactive.

A Brain magnetic resonance image



B Chest radiograph



Chest X-ray is shown. Two-dimensional echocardiography did not show any evidence of congenital heart disease. Arterial blood gas test results showed blood oxygen saturation of 80%. Blood culture results were sterile.

Q: Analyze and diagnose the most likely disease in this case.

Reference & Model Answers

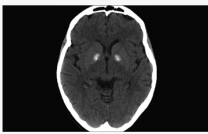
✦ Ground truth					
brain abscess	brain abscess	brain abscess	brain abscess	PAVM	brain abscess
	✓	✓	✓	✗	✓

PAVM:pulmonary arteriovenous malformation
*Core diagnostic results extracted from the diagnostic text generated by the model

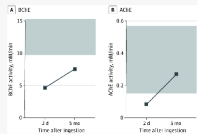
(c)

Level 2 Error Case

A 34-year-old man presented with a 1-month history of headache, diplopia, seizures, and altered consciousness for 1 week. The patient had had 2 seizures characterized by a tonic left deviation of the head and eyeballs, followed by brief tonic-clonic activity of the extremities, and confusion lasting 10 to 15 minutes after the seizure. The patient denied a history of fever, head trauma, limb weakness, or vomiting. The patient was a vegetarian and did not smoke or drink alcohol. The patient denied a history of drug addiction. Physical examination revealed that the patient was confused ... Liver and kidney function tests were normal. HIV enzyme-linked immunosorbent assay was unreactive.



A BCL6



Q: Analyze and diagnose the most likely disease in this case.

Reference & Model Answers

✦ Ground truth					
Organophosphate poisoning	carbon monoxide poisoning				
	✓	✓	✓	✓	✗

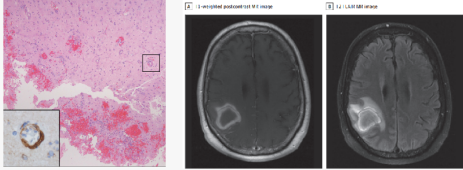
*Core diagnostic results extracted from the diagnostic text generated by the model

(d)

Figure 10: Additional error cases.

Level 2 Error Case

... ..intermittent headaches for several weeks, which progressed to severe persistent headaches with pain in the right eye. The patient had hypertension, hyperlipidemia, diabetes mellitus, and atrial fibrillation.... Neurologic examination revealed disorientation, short-term memory impairment, and left arm supination....Cerebrospinal fluid (CSF) examination showed normal red blood cell count, protein and glucose levels, and a mildly elevated white blood cell count of 11 cells/ μ L....



Q: Analyze and diagnose the most likely disease in this case.

Reference & Model Answers

Ground truth	MedGemini
Erdheim-Chester disease (ECD)	neoplastic process
Multiple Sclerosis	a low-grade glioma
a low-grade glioma	Glioblastoma

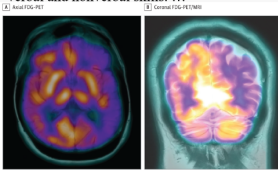
✗ ✗ ✗ ✗ ✗

*Core diagnostic results extracted from the diagnostic test generated by the model

(a)

Level 2 Error Case

A 44-year-old male was referred for progressive Parkinson's disease with poor response to levodopa. ... Over the past 2 years he has experienced worsening stiffness, difficulty walking, and frequent falls. He reported REM sleep behavior disorder, restless legs syndrome, daytime visual hallucinations, and rapid cognitive decline. ... He was treated with levodopa/benserazide (up to 200 mg/50 mg 4 times daily), but his Unified Parkinson's Disease Rating Scale score did not improve, so dopaminergic medication was discontinued. ... Neurologic examination showed reduced expression, symmetrical bradykinesia, and tetany, but no tremor. Eye movements were wide-ranging, with large sweeping disturbances during smooth tracking. Neuropsychological evaluation revealed significant abnormalities in cognitive functioning affecting both verbal and nonverbal skills. ...



Q: Analyze and diagnose the most likely disease in this case.

Reference & Model Answers

Ground truth	MedGemini
Autosomal recessive Parkinson's disease	Levy body dementia
Levy body dementia	DAP
acute ischemic stroke	Levy body dementia
Levy body dementia	Levy body dementia

✗ ✗ ✗ ✗ ✗

*Dementia associated with Parkinson's (DAP)

(b)

Level 2 Error Case

... ..was diagnosed with *Alzheimer's disease* after two years of progressive short-term memory loss due to persistent abnormal behavior, and an MRI scan of his brain showed hippocampal atrophy. His wife brought him to the neurology clinic. His medical history is characterized by well-controlled hypertension and type 2 diabetes mellitus. He did not have any personal or family history of mental illness. Patient's regular medications (levostigmine, 9.5 mg daily, transdermal; enalapril; metformin). ...began to experience the symptoms in the risk video. BMSE were 20 out of 30: orientation (-1), recording (-3), recall (-3), attention and continuity 7 out of 30. Electroencephalography, magnetic resonance imaging of the brain, and metabolic findings were unremarkable....



Q: Analyze and diagnose the most likely disease in this case.

Reference & Model Answers

Ground truth	MedGemini
Mirror Self Misidentification (MSD)	MSD
MSD	AD
AD	AD
AD	MSD

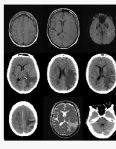
✓ ✗ ✗ ✗ ✓

*Core diagnostic results extracted from the diagnostic test generated by the model

(c)

Level 3 Error Case

Presents to ED with confusion and word finding difficulties. External CT - left MCA infarct with edema. Patient Data: Age: 75 years, Gender: Male



Q1: What is the most likely diagnosis based on the brain imaging?

Q2: What features in the image support the presence of vasogenic edema?

Q3: Based on the imaging features, does this lesion more likely represent a primary brain tumor or a metastasis?

Reference & Model Answers

Ground truth	MedGemini
Solitary brain metastasis in the left parieto-occipital region	Ischemic Stroke
Perilesional white matter shows hypoaattenuation	Low density of white matter around the lesion
Metastasis	Neither
	Surrounding low density shows vasogenic edema from blood-brain barrier disruption.
	Metastasis

● ● ●

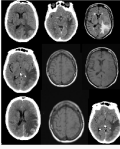
*Core diagnostic results extracted from the diagnostic test generated by the model

(d)

Figure 11: Additional error cases.

Level 3 Error Case

Q1: What is the most likely diagnosis based on the brain imaging?
Q2: What features in the image support the presence of vasogenic edema?
Q3: Based on the imaging features, does this lesion more likely represent a primary brain tumor or a metastasis?
Q4: Are there imaging features suggesting acute infarction, and how do they differ from the mass lesion?
Q5: Does the image suggest mass effect or herniation? If so, to what extent?



Reference & Model Answers

Ground truth	Model Answer 1	Model Answer 2
Solitary brain metastasis	Middle cerebral artery stroke	Acute deep grey infarction
Vasogenic edema, no shift	Perilesional edema, asymmetry	Hypodensity and mass effect
Metastasis over glioma	Ischemic stroke	Venous thrombosis suspected
Left MCA infarct	Venous thrombosis or hypertension	Indicate acute vascular pathology
Mild mass effect	Mild mass effect	Left MCA territory

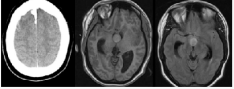
*Core diagnostic results extracted from the diagnostic text generated by the model

(a)

Level 3 Error Case

Presentation: Severe headaches for 4 months.
 Features of raised intracranial pressure.
 Age: 30 years
 Gender: Female

Q1: What is the most likely diagnosis based on the imaging features?
Q2: Which imaging feature best explains the patient's symptoms of raised intracranial pressure?
Q3: What imaging sign indicates transependymal CSF flow due to hydrocephalus?
Q4: What feature confirms that there is no downward herniation in this case?
Q5: What prior surgical intervention can be inferred from the imaging?



Reference & Model Answers

Ground truth	Model Answer 1	Model Answer 2
Colloidal cyst of the third ventricle.	Space-occupying brain tumor with obstructive hydrocephalus	???
Foramen of Monro cyst	Hydrocephalus with ventricular dilation	???
Transependymal edema	Periventricular hyperintensity	Periventricular transependymal edema
Normal fourth ventricle	No tentorial indentation	???
Bifrontal burr holes	No prior surgery evident	???

*Core diagnostic results extracted from the diagnostic text generated by the model

(b)

Figure 12: Additional error cases.